Intelligent Design Of UAV Unique Flight Route Scheme Based On Lidar Technology

Xun Wang[1], Xinyang Guo[1], Zilong Hou[1], Weijing Li[2] and Yi Ding[2, 3]

[1]Maintenance Branch of State Grid Ji Bei Electric Power Co., LTD., Beijing,102488, China;

[2]Biejing Zhongfei airwing Technology Co., LTD., Beijing 100176, China;

[3]The Experimental High School Attached To Beijing Normal University, Beijing, 100032, China;

Keywords: Lidar Technology; Uav Flight Path; Kalman Algorithm; Intelligent Design

Abstract: With the continuous development and maturity of sensor technology, laser technology and computer technology, airborne lidar measurement technology has become an important technical means to obtain three-dimensional spatial information. It can quickly and efficiently obtain accurate three-dimensional coordinates of objects and high-resolution digital terrain models. It has unique technical advantages and wide application prospects in building 3D modeling, forest survey, topographical mapping, pipeline laying design, coastline analysis and power line patrol. In this regard, the use of lidar technology to study the flight path of the UAV is of great significance. This article first introduces the sensor's working principle and device selection, and describes the IMU/DGPS integrated navigation principle. Then combined with the small unmanned helicopter model, the eleventh-order extended Kalman data fusion algorithm is designed and implemented. According to the characteristics of each sensor in the airborne lidar digital terrain mapping system, the role of the data fusion algorithm is analyzed. Finally, the experimental verification and analysis of the whole system are carried out. Studies have shown that when there is no DGPS update value, even if the DGPS data cannot be used due to external interference in a short period of time, the UAV flight route prediction system can obtain more accurate position information.

1. Introduction

UAV lidar technology is an emerging measurement technology that integrates high-precision dynamic DGPS technology, laser ranging technology, high-precision carrier attitude measurement technology and computer technology [1-2]. The distance information obtained by the laser rangefinder combined with the attitude information obtained by the attitude measurement module and the position information obtained by the high-precision differential GPS can be solved to obtain accurate three-dimensional coordinates of the object and a high-resolution digital terrain model [3-4]. It provides a new method of remote sensing technology for continuous and automatic acquisition of Earth's spatial information. Compared with the traditional manual single-point data acquisition method, UAV's unique flight route automation and intelligence have made a big step forward. The observation accuracy and speed are significantly improved [5-6].

At present, China has not developed a light and small airborne lidar system based on a small unmanned helicopter platform [7-8]. It is worth noting that our institute is actively organizing forces to build on light-weight design of existing equipment and key technologies of each unit based on the preliminary results of large-scale airborne lidar systems, and to build light and small airborne lidar System [9-10].

This article first briefly introduces the basic principles of the extended Kalman algorithm, then combines with a specific small unmanned helicopter model, designs and implements an eleventh-order extended Kalman algorithm, and gives an engineering feasible determination of the Kalman parameter matrix method. In this paper, the precise measurement of the width of the workpiece, the binarization of the image, the extraction of the region of interest and the outline of the image are achieved. The measurement experiments on the workpieces of different sizes are carried out to verify the practical availability of the visual measurement algorithm. Finally,

according to the characteristics of each sensor in the airborne lidar digital terrain mapping system, the role of data fusion algorithm is analyzed. This paper proposes a practical method for parameter selection in engineering practice in view of the difficult problem of algorithm parameter matrix selection. Finally, the function of the extended Kalman data fusion algorithm is analyzed according to the characteristics of the airborne lidar system sensor, and the simulation results of the actual experimental data are given.

2. Principle design of UAV flight route based on lidar technology

2.1 Composition of Airborne System

(1) Inertial navigation unit IMU

The speed of the airborne system is obtained by accumulating the acceleration of the aircraft over time. Assuming that the function of the acceleration of the airborne system along a certain axis with time is a(t), then the airborne system at a certain time in the direction of the axis t_k. The speed u(t) can be expressed as:

$$u(t_k) = u(t_0)a(t) + \int_{t_0}^{t_k} a(t)dt \quad (1)$$

Where u(t) is the speed of the airborne system at the initial moment. In actual application, this speed is the speed of the airborne system when it is powered on, which is generally zero.

When the airborne system is stationary or moving at a constant speed, the value obtained by the three-axis accelerometer is only generated by the projected component of the acceleration of gravity on each axis. In this way, the relationship between trigonometric functions can be used to obtain the roll angle and pitch angle of the airborne system when it is stationary or moving at a constant speed:

$$Roll = atan2(accel_y, accel_z) \quad (2)$$

$$Pitch = -asin2(accel_x, g) \quad (3)$$

Among them, Roll is the roll angle, Pitch is the pitch angle, and $accel_x$, $accel_y$, and $accel_z$ are the projections of the gravity acceleration g in the x, y, and z axis directions, respectively.

(2) Electronic compass

The magnetoresistive sensor is used to sense the earth's magnetic field. The tilt sensor can perform real-time compensation when the electronic compass is in a non-horizontal state. The micro-control system processes the signals of the magnetoresistive sensor and the tilt sensor and performs data calculation, compensation, and output.

2.2 Airborne Lidar Positioning Principle

Compared with DGPS technology, the advantages of IMU inertial navigation are obvious: it can obtain high-precision attitude information, but also speed and position information, and is a completely autonomous navigation module that is not affected by external environmental factors. Data The output frequency is very high. From the application point of view, one of the main disadvantages of IMU is that the error accumulates over time, and the single use cannot guarantee the correct operation for a long time, and it is determined by the material characteristics of the sensor and cannot be eliminated.

2.3 Application of Eleventh Order EKF Data Fusion Algorithm in Airborne System

In order to obtain accurate point cloud information and realize the navigation control of the unmanned helicopter, it is necessary to obtain the nonlinear mathematical model of the airborne platform. Select 3 position information (x, y, z), 3 speed information (u, v, w) of the system in the navigation coordinate system, the airborne system attitude information (q_0, q_1, q_2, q_3) and local gravity acceleration g described by quaternion as the state vector of the system. Select 3 position information (x, y, z), 3 velocity information (u, v, w), three airborne system attitude information (φ, ϕ, ψ) expressed by Euler angle as the system observation vector. In the selection of parameters here, the attitude angle expressed by the Euler angle will cause the singularity of the Euler angle equation when the attitude of the airborne platform changes greatly.

$$\begin{cases} \varphi = arctan2(2(q_2q_3 + q_0q_1), (1 - 2(q_1^2 + q_2^2))) \\ \theta = -\arcsin(2(q_1q_3 - q_0q_2)) \\ \psi = \arctan2(2(q_1q_2 + q_0q_3), (1 - 2(q_2^2 + q_3^2))) \end{cases} \tag{4}$$

The nonlinear navigation model of the small unmanned helicopter constructed in this paper is as follows:

$$\begin{cases} X = f(X(t), u(t), t) \\ Z(t) = h(X(t), t) \end{cases} \tag{5}$$

Among them:

$$X = [x \;\; y \;\; z \;\; u \;\; v \;\; w \;\; q_1 \;\; q_2 \;\; q_3 \;\; g]^T \tag{6}$$

State vector of the system.

$$Z = [x \;\; y \;\; z \;\; u \;\; v \;\; w \;\; \varphi \;\; \theta \;\; \psi]^T \tag{7}$$

The observation vector of the system.

2.4 Image Binarization Technology

(1) Histogram double peak method

The grayscale histogram of the image intuitively shows the distribution of the grayscale value of each pixel in the image. If the target area and the background area of the original image are single peaks, and the gray values of the pixels on both sides of the junction of the two areas are obviously different, then the gray value of the histogram valley point can be used as the threshold for segmenting the image.

(2) Optimal iteration threshold method

When the gray values of the target and background areas in the image are interlaced with each other, the use of estimated values for segmentation will inevitably cause corresponding errors. In order to reduce the error segmentation rate, iterative threshold method can be used to find the threshold.

3. Design of experimental plan of UAV flight route based on lidar technology

3.1 Experimental Scheme Design

Choose an open space without occlusion. The simulation experiment in this paper selects the roof of the building to ensure the normal operation of DGPS. Then put a cylindrical water pipe with a length of more than 2 meters and a diameter of 15 centimeters at a fixed position on it, and place obvious control points around the water pipe. The two carried the unmanned helicopter along the direction of the water pipe. At this time, the airborne system was about two meters above the ground, allowing the airborne lidar system to scan the water pipe and its surrounding features. There will be shaking during the process of carrying an unmanned helicopter. The airborne system must be able to obtain the true attitude of the airborne system during this process, otherwise it will not be possible to obtain the correct 3D point cloud. During the experiment, you can increase the jitter of the simulated aircraft during flight according to the needs of the experiment, or you can let the drone scan the water pipe at a specific attitude angle. In the experiment, the speed of the airborne system is about 0.3m/s, the moving distance of the experimental system is about 5m, and the height is about 2m. The spot diameter of the laser rangefinder on the water pipe is about 4cm.

3.2 UAV Flight Route Process

When carrying out field experiments with an airborne lidar system, you need to follow the operation flow:

(1) Outfield planning: the flight site for actual measurement needs to be selected as an open place with typical topographical features, and the area of the site meets the flight requirements.

(2) Aircraft preparation: Before the flight experiment, power on the steering gear and check whether the steering gear responds normally and the action logic is correct. Check whether the oil volume of the oil tank is sufficient to meet the needs of the experiment, and add an appropriate amount of fuel to the oil tank. Start the electronic cabin before starting the engine, and test the

whole machine on the ground to eliminate the problem.

(3) Erection and configuration of base station/ground station: Before starting the experiment, you need to erect the GPS reference station according to the instructions in the system operation manual; start the ground station server, open the 3D terrain system software, connect to the network, and cooperate with the airborne system for testing, Mainly configure the network and test the network response.

(4) Trajectory planning: Trajectory planning is mainly based on the experimental site, setting the flight path and flight speed of the aircraft, and setting the flight path reasonably can collect more key information about the terrain.

(5) Data storage and display: During the flight of the aircraft, the data is transmitted back to the ground station system in real time. The system software saves the data sent back by the airborne lidar system and processes the data to generate a point cloud image in real time.

(6) Map export: After the experiment, according to the needs of engineering design, output a data file that conforms to the format required by the project.

4. Experimental analysis of UAV flight route based on lidar technology

4.1 Experimental Analysis of UAV Flight Route

In order to verify the practicability of the system constructed in this paper and the accuracy of the three-dimensional point cloud data obtained by scanning, the control point is used to evaluate the accuracy. First, select three of the foot points as control points. During the experiment, the person carried the airborne system and scanned from right to left along the direction of the water pipe. The laser spot diameter of each control point was about 4 cm. The three control points are measured to obtain the precise latitude and longitude information of the three control points. After conversion, the real coordinate values of the control points under the END coordinate system unified with the airborne lidar system are obtained. By actually scanning the experimental scene, the measured coordinate values of the three control points can be obtained. The accuracy is evaluated by comparing the measured value of the control point with the true value error. As shown in Table 1, the measured value in the table is the average value of the control points obtained during the 10 experiments.

Table 1. Control point NED coordinates and error value

Control point number	True value END coordinates (m)	Measured value END coordinates (m)	Error value (m)
Number 1	(-0.324,6.746,4.375)	(-0.326,6.763,4.352)	(0.002, -0.017,0.023)
Number 2	(-0.846, -7.354,4.735)	(-0.863, -7.336,4.753)	(0.017, -0.018, -0.018)
Number 3	(0.628, -10.464,4.194)	(0.664, -10.425,4.164)	(-0.036, -0.039,0.030)

It can be seen from Table 1 that the END coordinate values of control points 1 and 3 have an error value of 2 cm in the north and east directions, and an error value of 1 cm in the ground direction. The accuracy of the control point 2 in the three axes is within 4cm. The reason for this difference is: the original point of this article is to select the top midpoint of the chair (upper surface diameter 224mm, lower surface 279mm, height 217mm) as the control point, but There is a hole with a diameter of 30mm in the middle, which reduces the measurement accuracy of the laser spot, which also verifies the accuracy of the system from the side. The selected control points confirm that the 3D point cloud data scanned by the system has high accuracy, and verify the correctness of the airborne laser measurement system and data fusion algorithm constructed in this paper.

4.2 Experimental Analysis of UAV Flight Path

The effect of eleven-order extended Kalman data fusion algorithm on the position information data fusion in this flight experiment is shown in Figure 1.

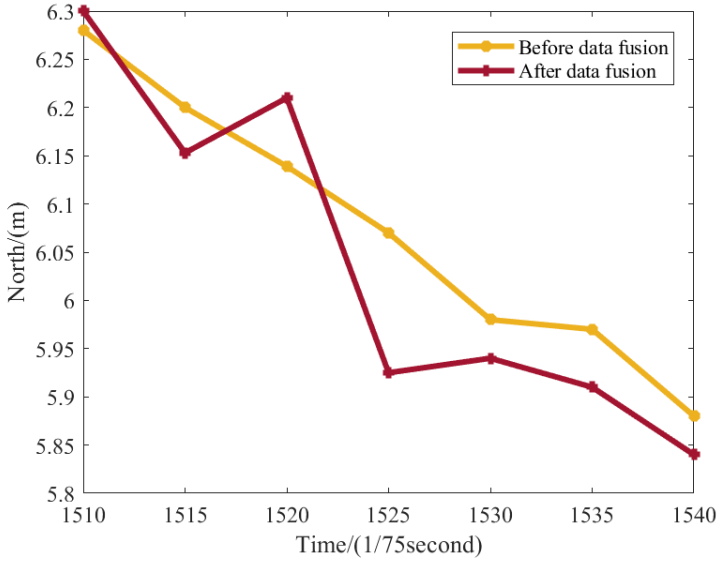

Figure 1. Fusion of northbound coordinate data

From Figure 1, we can see the effect of the eleventh-order extended Kalman data fusion algorithm on the position information of DGPS on a small unmanned helicopter platform. The update frequency of DGPS is 20Hz, which is less than the sampling frequency of the coprocessor module to the IMU is 75Hz. The DGPS data before the data fusion is a stepwise mutation. The system uses the updated DGPS data to correct the predicted value of the IMU sensor when the DGPS data has an updated value. When there is no DGPS updated value, only the three-axis acceleration and the IMU are used. Three-axis angular velocity information to predict the position value of the airborne system. In this way, even if the DGPS data cannot be used due to external interference within a short period of time, relatively accurate position information can be obtained.

Conclusions

The multi-sensor data synchronization mechanism constructed in this paper uses hardware design and software to achieve synchronization to add accurate time attributes to different sensor data. This time attribute is transmitted along with the sensor data and is solved according to this time attribute in the ground station system. data. This paper implements an eleventh-order extended Kalman data fusion algorithm for small unmanned helicopter platforms, effectively fuse data from various sensors, overcomes the shortcomings of sensors, and provides a basis for obtaining high-precision point cloud data.

Project

Research and Application of Autonomous Inspection Technology of Unmanned Aerial Vehicle Formation for Overhead Transmission Lines
Description code: 5200-201918066A-0-0-00

References

[1] R. Shahrin M , H. Hashim F , M. D W Z W , et al. 3D indoor mapping system using 2D LiDAR sensor for drones[J]. International Journal of Engineering and Technology, 2018, 7(4.11):179-183.

[2] Murtha T M , Broadbent E N , Golden C , et al. Drone-Mounted Lidar Survey of Maya Settlement and Landscape[J]. Latin American Antiquity, 2019, 30(3):630-636.

[3] Sprowl B . PRECISIONHAWK USES DRONE TECHNOLOGY TO HUNT FOR BURIED TREASURE INTHE PHILIPPINES[J]. Unmanned Systems, 2019, 37(3):42-43.

[4] Behroozpour B , Sandborn P A M , Wu M C , et al. Lidar System Architectures and Circuits[J]. IEEE Communications Magazine, 2017, 55(10):135-142.

[5] Babahajiani P , Fan L , Kämäräinen, Joni Kristian, et al. Urban 3D segmentation and modelling from street view images and LiDAR point clouds[J]. Machine Vision & Applications, 2017, 28(7):679-694.

[6] Guerra E , Munguia R , Bolea Y , et al. Detection and Positioning of Pipes and Columns with Autonomous Multicopter Drones[J]. Mathematical Problems in Engineering, 2018, 2018(pt.7):2758021.1-2758021.13.

[7] Watts A . 3D printing presents industry opportunities[J]. Consulting-specifying engineer, 2019, 56(4):11-11.

[8] Ahmad Z A , Guey C W , Sze L T , et al. Scalable and Cost Effective High Resolution Digital Elevation Model Extraction Method for Slope's Stability Assessment[J]. Advanced Science Letters, 2017, 23(2):1289–1293.

[9] Xing Z , Xia Y . Comparison of centralised scaled unscented Kalman filter and extended Kalman filter for multisensor data fusion architectures[J]. IET Signal Processing, 2016, 10(4):359-365.

[10] Jens H , Harald B . Lidar as a key technology for automated and autonomous driving[J]. Atz Worldwide, 2018, 120(S1):70-73.